

# The Experimental Manifestations of Corner-Cutting Tunneling<sup>1</sup>

Yongho Kim and Maurice M. Kreevoy\*

Contribution from the Chemical Dynamics Laboratory, Department of Chemistry, University of Minnesota, 207 Pleasant Street SE, Minneapolis, Minnesota 55455. Received October 31, 1991

**Abstract:** A family of potential energy surfaces has recently been developed, based on a linear, 3-body model, which permits the calculation of rate constants that accurately mimic a large body of data for hydride transfer reactions in solution. Two of the parameters of the symmetrical surface have now been systematically varied so as to alter the importance of hydrogen tunneling, and the effects on measurable parameters have been examined. On all reasonable variants of the surface, at temperatures  $\sim 300$  K, most hydride transfer events occur by tunneling, and tunneling generally accounts for a large fraction of deuteride and tritide transfer events as well. At this temperature most tunneling occurs at donor-acceptor distances slightly larger than those of the transition states (corner-cutting). Tunneling increases the rate of hydride transfer by about a factor of 10. The isotopic difference in Arrhenius activation energies,  $E_a(D) - E_a(H)$ , is increased by about 1 kcal mol<sup>-1</sup> and the ratio of preexponential factors,  $A(H)/A(D)$ , is reduced by tunneling. However, it appears that completely unambiguous experimental proof that tunneling occurs would be impossible to obtain at  $\sim 300$  K, although tunneling becomes clearly evident at much lower temperatures. The commonly observed steric magnification of the kinetic isotope effect requires no special modification of the potential energy surface. It can be reproduced by increasing the equilibrium donor-acceptor distance. It is partly due to tunneling and partly due to isotopic differences in the variational transition states. An increase in kinetic isotope effect when the hydride donor is modified so as to increase the equilibrium constant is a symptom of tunneling. The most reliable experimental indications of tunneling obtainable at  $\sim 300$  K are probably a combination of these effects, without significant exceptions. In systems with only one isotopically substituted hydrogen, the Swain-Schaad relation appears to hold as well in the presence of tunneling as in its absence. It appears to be a reliable way of estimating a tritium isotope effect from the corresponding deuterium isotope effect, but it is not useful for identifying the origin of the effects.

## 1. Introduction

The importance of tunneling in chemical reactions has been discussed for many years.<sup>2</sup> The focus of much of this work has been an attempt to unambiguously prove the occurrence of tunneling. In fact, tunneling is not a new or independent physical phenomenon. It is generally to be expected in molecular quantum mechanics, just as zero-point energy is expected. It can generally be expected to play a significant role in the passage of finite barriers by systems with effective mass of one or a few daltons. In this paper we try to identify observables which will be altered in predictable ways by tunneling.

A less well known but related problem concerns the structure of the critical configuration—defined as the most probable structure for crossing the surface that separates reactants from products in potential energy hyperspace.<sup>3</sup> Variational transition state theory<sup>4-7</sup> has repeatedly been shown to give a better approximation of rate constants than conventional transition state theory.<sup>4-8</sup> In variational transition state theory it is the dividing surface of maximum Gibbs free energy,  $G$ , rather than the point of maximum potential energy,  $V$ , on the minimum energy path (MEP) from reactants to products that is identified as the transition state. Because structurally and isotopically sensitive zero-point energies and partition functions contribute to  $G$ , the dividing surface that defines the variational transition state often

does not pass through the potential energy saddle point (conventional transition state).<sup>4-7</sup> In those cases the variational transition state usually also changes slightly under isotopic substitution, even though the potential energy,  $V$ , is assumed to be invariant under isotopic substitution (Born-Oppenheimer approximation).<sup>9</sup> The usual outcome, in cases where the variational transition state is different from the conventional transition state, is that the light transition state is further from the potential energy saddle point than the heavy transition state; the calculated rate constant for the light variant of the reaction,  $k$ , is reduced more by using the variational transition state than by using the rate constant for the heavy variant,  $k'$ . If the calculations are being used to elucidate experimental results, and the kinetic isotope effect (KIE) is being forced to match the experimental values, the quasiclassical KIE is normally reduced, and the tunneling contribution to the KIE is increased, by using variational transition state theory.<sup>4-7</sup>

In the present paper we examine the nature of the reactive processes and the effectiveness of various experimental criteria for detecting departure from conventional, quasiclassical behavior. The criteria which we examine include the magnitude of several quantities derived from the temperature dependence of the KIE,<sup>2,10</sup> the value of the exponent,  $r$ , in the Swain-Schaad relation (eq 1),<sup>11,12</sup> and the response of the KIE to changes in the reaction equilibrium constant, produced by systematically changing the structure of one or the other of the reactants.<sup>3,13</sup>

$$k_H/k_T = (k_H/k_D)^r \quad (1a)$$

$$k_H/k_T = (k_D/k_T)^{r/(r-1)} \quad (1b)$$

Previous examinations of the validity of these criteria have been handicapped by the lack of potential energy surfaces which were reliable in the neighborhood of the saddle point. We have now developed a family of global potential energy surfaces based on a collinear, 3-body model for hydride transfer between NAD<sup>+</sup> analogues.<sup>14</sup> An atom of mass 1, 2, or 3 dalton is transferred

(1) This work was supported in part by the U.S. National Science Foundation, through Grant No. CH89-00103, and, in part, by a grant of computing time from the Minnesota Supercomputer Institute.

(2) Bell, R. P. *The Tunnel Effect in Chemistry*; Chapman and Hall: New York, 1980; pp 88-91 and 106-144.

(3) Kreevoy, M. M.; Ostović, D.; Truhlar, D. G.; Garrett, B. C. *J. Phys. Chem.* **1986**, *90*, 3766.

(4) Truhlar, D. G.; Isaacson, A. D.; Garrett, B. C. In *Theory of Chemical Reaction Dynamics*; Baer, M., Ed.; CRC Press: Boca Raton, FL, 1985; Vol. 4, p 65.

(5) Garrett, B. C.; Truhlar, D. G.; Wagner, A. F.; Dunning, T. H. *J. Chem. Phys.* **1983**, *78*, 4400.

(6) Garrett, B. C.; Abusalbi, N.; Kouri, D. J.; Truhlar, D. G. *J. Chem. Phys.* **1985**, *83*, 2252.

(7) (a) Garrett, B. C.; Joseph, T.; Truong, T. N.; Truhlar, D. G. *Chem. Phys.* **1989**, *136*, 271. (b) Lu, D.-H.; Truong, T. N.; Melissas, V. S.; Lynch, G. C.; Lieu, Y.-P.; Garrett, B. C.; Steckler, R.; Isaacson, A. D.; Rai, S. N.; Hancock, G. C.; Lauderdale, J. G.; Joseph, T.; Truhlar, D. G. *Computer Phys. Comm.*, submitted for publication.

(8) Glasstone, S.; Laidler, K. J.; Eyring, H. *The Theory of Rate Processes*; McGraw-Hill: New York, 1941; p 196.

(9) Born, M.; Oppenheimer, J. R. *Ann. Phys.* **1927**, *84*, 457.

(10) Shiner, V. J.; Smith, M. L. *J. Am. Chem. Soc.* **1961**, *83*, 593.

(11) Swain, C. G.; Stivers, E. C.; Reuwer, J. F.; Schaad, L. J. *J. Am. Chem. Soc.* **1958**, *80*, 5885.

(12) Lewis, E. S.; Robinson, J. K. *J. Am. Chem. Soc.* **1968**, *90*, 4337.

(13) Kreevoy, M. M.; Lee, I.-S. H. *Z. Naturforsch.* **1989**, *44*, 418.

between two atoms of mass 15 daltons. These potential energy surfaces were forced to reproduce the Marcus parameters and KIE values derived from a large number of rate constants and equilibrium constants for hydride transfers between NAD<sup>+</sup> analogues in solution. The large body of data which this potential function has allowed us to mimic suggests that its general characteristics have some validity.

The potential function is given by eq 2, where  $V_{\text{ELEPS}}$  is an extended LEPS potential function,<sup>15</sup>  $V_{\text{CD}}$  is a potential function for charge-induced dipole interaction,<sup>14</sup>  $V_{\text{solv}}$  is the generalized Born equation for the solvation of a charged molecule in a dielectric continuum,<sup>16-19</sup> and  $V_{\text{W}}$  is an arbitrary function introduced

$$V = V_{\text{ELEPS}} + V_{\text{CD}} + V_{\text{solv}} + V_{\text{W}} \quad (2)$$

to make the potential surface flatter near the saddle point and the critical complex, to obtain reasonable isotope effects.<sup>20</sup> The structure and energy at the reactants, products, and saddle point are not changed by  $V_{\text{W}}$ .<sup>14</sup> In order to change the tunneling effect on the rates, we vary a parameter of the widening function or the equilibrium C-C distance, without changing any other potential function parameters. A detailed description of the potential function was reported in a previous paper.<sup>14</sup>

## 2. Calculations

Rates are calculated by eq 3a, which implements the canonical variational transition state theory, or by eq 3b, which implements conven-

$$k^{\text{CVT}} = \kappa \left( \frac{k_{\text{B}}T}{h} \right) \left\{ \frac{Q^{\text{GT}}(\text{T},s)}{Q^{\text{R}}(\text{T})} \right\} \exp \left\{ - \frac{\Delta V_{\text{a}}^{\text{G}}(s)}{k_{\text{B}}T} \right\} \quad (3a)$$

$$k^{\ast} = \kappa \left( \frac{k_{\text{B}}T}{h} \right) \left\{ \frac{Q^{\ast}(\text{T})}{Q^{\text{R}}(\text{T})} \right\} \exp \left\{ - \frac{\Delta V_{\text{a}}^{\ast\text{G}}}{k_{\text{V}}T} \right\} \quad (3b)$$

$$Q^{\text{GT}}(\text{T},s) = Q_{\text{e}}^{\text{GT}}(\text{T}) Q_{\text{v}}^{\text{GT}}(\text{T},s) Q_{\text{r}}^{\text{GT}}(\text{T},s) \quad (4)$$

$$Q^{\text{R}}(\text{T}) = \Phi_{\text{rel}}^{\text{A,B}}(\text{T}) Q^{\text{A}}(\text{T}) Q^{\text{B}}(\text{T}) \quad (5)$$

$$V_{\text{a}}^{\text{G}}(s) = V_{\text{MEP}}(s) + \sum_n \epsilon_n(s) \quad (6)$$

$$\Delta V_{\text{a}}^{\text{G}}(s) = V_{\text{a}}^{\text{G}}(s) - V_{\text{a}}^{\text{G}}(s=-\infty) \quad (7)$$

tional transition state theory.<sup>4-7,21,22</sup> The  $Q^{\ast}$ 's are analogues of the related quantities in eq 3a, but evaluated at the saddle point.  $\Delta V_{\text{a}}^{\ast\text{G}}$  is  $\Delta V_{\text{a}}^{\text{G}}(s=0)$ .  $Q^{\text{GT}}(\text{T},s)$  is the partition function of the generalized transition state in mass-scaled orthogonal coordinates,  $Q^{\text{R}}(\text{T})$  is the partition function of the reactants, and  $\Phi_{\text{rel}}^{\text{A,B}}(\text{T})$  is the relative translational partition function per unit volume.  $Q_{\text{e}}^{\text{GT}}(\text{T})$ ,  $Q_{\text{v}}^{\text{GT}}(\text{T})$ , and  $Q_{\text{r}}^{\text{GT}}(\text{T})$  are the electronic, vibrational, and rotational partition functions at the generalized transition state, respectively.  $Q^{\text{A}}(\text{T})$  and  $Q^{\text{B}}(\text{T})$  are the non-translational parts of the partition functions of the two reactants. They are made up in the same way as  $Q^{\text{GT}}$ . The electronic partition function is always unity in the present calculations, but it is included for generality. The vibrational partition functions in eqs 4 and 5 are evaluated by using eq 8 and taking the lowest allowed vibrational level as the zero of energy. The rotational partition function for the linear molecule is given by eq 9 where  $I$  is the moment of inertia.  $V_{\text{a}}^{\text{G}}(s)$  is the vibrationally adiabatic

$$Q_{\text{v}}^{\text{GT}}(\text{T}) = \prod_m \left\{ 1 - \exp \left( - \frac{h\nu_m}{k_{\text{B}}T} \right) \right\}^{-1} \quad (8)$$

$$Q_{\text{r}}^{\text{GT}}(\text{T}) = \frac{2Ik_{\text{B}}T}{h^2} \quad (9)$$

ground-state energy at various points on the minimum energy path from reactants to products (MEP) and  $\epsilon_n$  is the zero-point energy of vibrational

(14) Kim, Y.; Truhlar, D. G.; Kreevoy, M. M. *J. Am. Chem. Soc.* **1991**, *113*, 7837.

(15) Kuntz, P. J.; Nemeth, E. M.; Polanyi, J. C.; Rosner, S. D.; Young, C. E. *J. Chem. Phys.* **1966**, *44*, 1168.

(16) Hoihtink, G. J.; de Boer, E.; van der Meij, P. H.; Weijland, W. P. *Recl. Trav. Chim. Pays-Bas.* **1956**, *75*, 487.

(17) Chalvet, O.; Jano, I. C. R. *Seances Acad. Sci.* **1965**, *261*, 103.

(18) Kozaki, T.; Morihashi, K.; Kikuchi, O. *J. Am. Chem. Soc.* **1989**, *111*, 1547.

(19) Tucker, S. C.; Truhlar, D. G. *Chem. Phys. Lett.* **1989**, *57*, 164.

(20) Truhlar, D. G.; Horowitz, C. J. *J. Chem. Phys.* **1978**, *68*, 2466.

(21) Truhlar, D. G.; Garrett, B. C. *J. Chim. Phys.* **1987**, *84*, 365.

(22) Garrett, B. C.; Truhlar, D. G.; Grev, R. S.; Magnuson, A. W. *J. Phys. Chem.* **1980**, *84*, 1730.

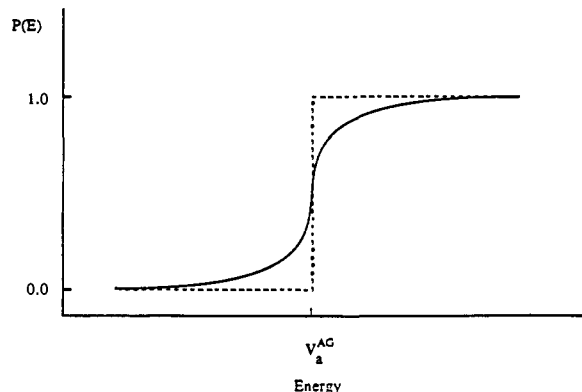


**Figure 1.** The quasiclassical (dashed line) and quantum mechanical (solid line) transmission probabilities,  $P(E)$ , as a function of energy. In quasiclassical variational transition state theory a system moving from reactants toward products along the minimum energy path has unit probability of crossing into the product valley if its energy is greater than  $V_{\text{a}}^{\text{AG}}$ , the sum of the potential energy plus the vibrational zero-point energy at the variational transition state. If its energy is less than  $V_{\text{a}}^{\text{AG}}$ , it has zero probability of crossing. When quantum mechanics is used,  $P(E)$  is not exactly zero for any energy and rises toward 0.5 as the energy approaches  $V_{\text{a}}^{\text{AG}}$ . For energies just above  $V_{\text{a}}^{\text{AG}}$ ,  $P(E)$  is still significantly below 1.0.

mode  $n$ . Variational transition state theory differs from conventional transition state theory in that  $\Delta V_{\text{a}}^{\text{G}}$  and the partition functions which enter eq 3 are evaluated at the variational transition state, defined as the generalized transition state for which  $s = s_{\text{min}}$ , that minimizes  $k^{\text{CVT}}$  (eq 3a). In conventional transition state theory they are evaluated at the potential energy saddle point.<sup>4-7</sup>

The transmission coefficient is  $\kappa$ . It is the ratio of the thermally averaged quantum transmission probability to the thermally averaged classical transmission probability, obtained by the large curvature ground state (LCG3) tunneling approximation.<sup>4,7,21</sup> The percentage of reactive events involving tunneling,  $P_{\text{T}}$ , can be calculated with this transmission coefficient by eqs 10 and 11, where  $V_{\text{a}}^{\text{AG}}$  is the maximum for the vibra-

$$\kappa = \kappa(V_{\text{a}}^{\text{G}} < V_{\text{a}}^{\text{AG}}) + \kappa(V_{\text{a}}^{\text{G}} \geq V_{\text{a}}^{\text{AG}}) \quad (10)$$

$$P_{\text{T}} = \{ \kappa(V_{\text{a}}^{\text{G}} < V_{\text{a}}^{\text{AG}}) / \kappa \} \times 100 \quad (11)$$

tionally adiabatic ground-state energy on the minimum energy path from reactants to products.  $\kappa(V_{\text{a}}^{\text{G}} < V_{\text{a}}^{\text{AG}})$  is the transmission coefficient including only contributions from energies below  $V_{\text{a}}^{\text{AG}}$ , and  $\kappa(V_{\text{a}}^{\text{G}} \geq V_{\text{a}}^{\text{AG}})$  is that including only contributions from energies at or above  $V_{\text{a}}^{\text{AG}}$ . The energy dependency of the quantal and classical transmission probability is shown in Figure 1. The contribution to the transmission coefficient for energy above  $V_{\text{a}}^{\text{AG}}$  is not due to the tunneling effect. Only that from configurations with energies below  $V_{\text{a}}^{\text{AG}}$  is attributed to the tunneling process. Equation 11 gives a slightly different value of  $P_{\text{T}}$  than eq 12 would give because, as shown in Figure 1,

$$P_{\text{T}} = 100(k - k_{\text{qc}}) / k \quad (12)$$

$\kappa(V_{\text{a}}^{\text{G}} \geq V_{\text{a}}^{\text{AG}})$  is less than the quasiclassical value of unity when the energy is equal to or only slightly more than  $V_{\text{a}}^{\text{AG}}$ . If  $\kappa$  were omitted from eqs 3a and 3b, the right-hand sides would define  $k_{\text{qc}}^{\ast}$  and  $k_{\text{qc}}^{\text{CVT}}$ .

The transmission coefficient is given by eqs 13, where  $E$  is the total

$$\kappa(\text{L}) = \frac{1}{k_{\text{B}}T} \exp \left\{ \frac{V_{\text{a}}^{\text{AG}}(\text{L})}{k_{\text{B}}T} \right\} \int_0^{\infty} P^{\text{G}}(\text{L}, E) \exp \left( - \frac{E}{k_{\text{B}}T} \right) dE \quad (13a)$$

$$= \frac{1}{k_{\text{B}}T} \int_0^{\infty} P^{\text{G}}(\text{L}, E) \exp \left( \frac{V_{\text{a}}^{\text{AG}}(\text{L}) - E}{k_{\text{B}}T} \right) dE \quad (13b)$$

energy,  $P(\text{L}, E)$  is the ground-state transmission probability, and L = H for hydrogen, D for deuterium, and T for tritium. The ground-state transmission probability is obtained by the large curvature ground state tunneling method (LGC3),<sup>4-7</sup> in which the tunneling path maximizes corner-cutting.

If we rewrite the KIE using eqs 3, we get the following equations, where L is D or T.

$$\frac{k_{\text{H}}}{k_{\text{L}}} = \frac{\kappa(\text{H}) Q^{\text{GT}}(\text{H}, \text{T}, s_{\text{min}}) Q^{\text{R}}(\text{L}, \text{T})}{\kappa(\text{L}) Q^{\text{GT}}(\text{L}, \text{T}, s_{\text{min}}) Q^{\text{R}}(\text{H}, \text{T})} \exp \left( \frac{\Delta \Delta E(\text{L})}{k_{\text{B}}T} \right) \quad (14)$$

$$\Delta \Delta E(\text{L}) = [V_{\text{a}}^{\text{R}}(\text{H}) - V_{\text{a}}^{\text{R}}(\text{L})] - [V_{\text{a}}^{\text{G}}(\text{H}) - V_{\text{a}}^{\text{G}}(\text{L})] \quad (15)$$

**Table I.** Conventional and Variational Transition State Theory Quasiclassical Rate Constants for Various Barrier Curvatures at 300 K

surface	$A_w$ , kcal mol <sup>-1</sup> A <sup>-6</sup>	$V_i(H)$ , <sup>a</sup> cm <sup>-1</sup>	$10^4 k_{H,qc}^*$ , M <sup>-1</sup> s <sup>-1</sup>	$10^4 k_{H,qc}^{CVT}$ , <sup>b</sup> M <sup>-1</sup> s <sup>-1</sup>	$10^4 k_{D,qc}^*$ , M <sup>-1</sup> s <sup>-1</sup>	$10^4 k_{D,qc}^{CVT}$ , <sup>c</sup> M <sup>-1</sup> s <sup>-1</sup>	$10^4 k_{T,qc}^*$ , <sup>b</sup> M <sup>-1</sup> s <sup>-1</sup>	$10^4 k_{T,qc}^{CVT}$ , <sup>c</sup> M <sup>-1</sup> s <sup>-1</sup>	$r_{qc}^{CVT,d}$
I	88.9	825	23.90	8.415	6.117	4.521	3.222	3.174	1.57
II	83.1	989	23.90	10.66	6.117	5.987	3.222	3.222	2.08
III	77.4	1130	23.90	14.96	6.117	6.117	3.222	3.222	1.73
IV	71.7	1254	23.90	23.23	6.117	6.117	3.222	3.222	1.48
V	66.0	1368	23.90	23.90	6.117	6.117	3.222	3.222	1.47
VI <sup>e</sup>	88.9	924	1118	471.7	253.7	253.7	152.9	152.6	1.82

<sup>a</sup>The imaginary frequency at the saddle point, with H as the transferred atom. Within a few percent,  $V_i(D)$  and  $V_i(T)$  are given by  $(\mu_H/\mu_L)^{1/2}V_i(H)$ , where  $\mu_L$  is the reduced mass of A-L, with an atomic weight of 15 daltons for A and a mass of 1, 2, or 3 daltons for L. <sup>b</sup>Calculated from eq 3b, omitting  $\kappa$ . <sup>c</sup>Calculated from eq 3a, omitting  $\kappa$ . <sup>d</sup>Quasiclassical, conventional transition state theory gives  $r_{qc}^* = 1.47$  for all the surfaces. <sup>e</sup>The same as surface II, except that  $\Delta G^\circ = -5$  kcal mol<sup>-1</sup>. Our method of varying  $\Delta G^\circ$  is described in ref 14.

**Table II.** Transmission Coefficients, Percentages of Tunneling, and Complete Swain-Schaad Ratios at 300 K

surface	$\kappa_H$	$P_T^H$	$\kappa_D$	$P_T^D$	$\kappa_T$	$P_T^T$	$r^{*a}$	$r^*$	$r^{CVT}$
I	2.83	81	1.23	41	1.11	27	1.13	1.34	1.32
II	5.32	91	1.54	56	1.43	49	1.06	1.27	1.38
III	7.18	93	2.31	72	1.81	60	1.22	1.35	1.44
IV	10.5	96	3.37	80	1.99	62	1.46	1.47	1.47
V	18.5	97	4.35	84	2.05	63	1.52	1.50	1.50
VI	3.75	86	1.46	51	1.31	43	1.12	1.32	1.40

<sup>a</sup>Defined by an equation analogous to eq 1, but with  $\kappa$ 's substituted for  $k$ 's.

The difference in zero-point-corrected potential energy between isotopic variants of the reactants is  $\Delta V_a^{RG}$ , defined in eq 16, since the same potential energy surface is used for all the isotopic variants.<sup>9</sup>

$$\Delta V_a^{RG} = V_a^{RG}(H) - V_a^{RG}(L) \quad (16)$$

### 3. Results and Discussion

We first examined the effect of changing the saddle point imaginary frequency by modifying the preexponential parameter of the widening function, given by eq 17. The  $r_{CH}^*$  values are the

$$V_w = A_w \frac{(r_{C_1H}^* r_{C_2H} - r_{C_2H}^* r_{C_1H})^2}{(r_{C_1H}^* + r_{C_2H}^*)^2} (r_{C_1H}^* r_{C_2H} + r_{C_2H}^* r_{C_1H})^2 \exp\left\{-\beta_w \left(\frac{r_{C_1H}^* r_{C_2H} + r_{C_2H}^* r_{C_1H}}{r_{C_1H}^* + r_{C_2H}^*}\right)^4\right\} \quad (17)$$

C-H distances at the saddle point, which are determined in a preliminary calculation without the widening function;  $A_w$  and  $\beta_w$  are adjustable parameters.  $C_1$  and  $C_2$  each have mass of 15 daltons but otherwise have the properties of carbon atoms. The value of  $A_w$  has been varied to obtain the different imaginary frequencies at the saddle point, and  $\beta_w = 0.47 \text{ \AA}^{-4}$ . The exponential term in eq 17 causes  $V_w$  to die off when either C-H distance is large, and the preexponential term makes the widening function zero at the saddle point even though the reaction is not symmetric.

Quasiclassical rate constants given by variational and conventional transition state theory are given in Table I. Table II shows the transmission coefficients and percentage tunneling (eq 11) for each surface and the Swain-Schaad exponent for conventional and for variational transition state theory ( $r^*$  and  $r^G$ ). It also shows the factor ( $r^{*a}$ ) which the  $\kappa$ 's contribute to both  $r^*$  and  $r^G$ . For hydride transfer, most reactive events occur by tunneling on all our surfaces. Even in surface I, which is the fattest near the saddle point, the critical configuration,  $P_T$ , is 80 for hydride transfer and substantial for deuteride and tritide transfer. Even when H is replaced by D or T,  $P_T$  remains above 50 in most cases, contrary to some previous estimates.<sup>12</sup> However, the fraction of the barrier which is avoided by tunneling is small; tunneling occurs close to the saddle point. It is also noteworthy that the hydrogenic vibrations are constrained to remain in their ground state throughout the transformation, in these calculations, but if this constraint is removed, the excitation of the hydrogenic vibrations remains unimportant.<sup>14</sup> The excitation which brings the reactants up to reactive configurations is in the low-frequency mode which represents the compression of the reactants and the

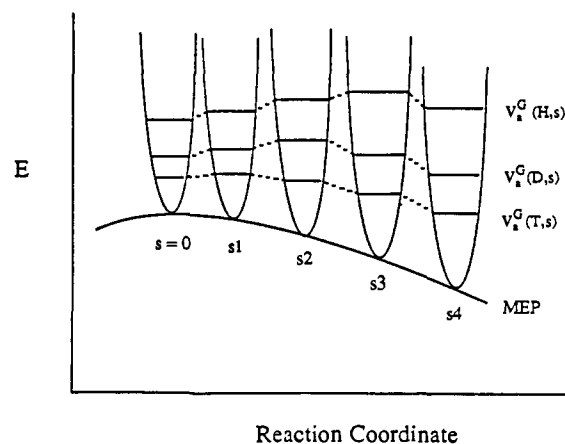


**Figure 2.** Conventional transition state theory locates the transition state at the point of maximum potential energy on the minimum energy path from reactants to products. Variational transition state theory locates the transition state at the point of maximum Gibbs free energy. If the present systems are on the minimum energy path and close to the potential energy saddle point their Gibbs free energies differ from their potential energies almost entirely by the zero-point energy in their three vibrational degrees of freedom. The zero-point energy increases as the system leaves the potential energy maximum, and may increase faster than the potential energy decreases if the maximum is not too sharp. Since the zero-point energy decreases in the order  $H > D > T$ , the three variational transition states will then occur at different values of  $s$ . This figure illustrates the point using a single vibrational degree of freedom.

reorganization of solvent. However, there is some reduction of the force constant of the hydrogenic mode as reactive configurations are approached.

As noted above, the variational transition state is not necessarily at the saddle point of the potential energy surface and not necessarily the same for H, D, and T transfer. This is shown in Figure 2. The variational transition states for H, D, and T transfer appear at  $s_3$ ,  $s_2$ , and  $s_1$  on the MEP, respectively. The vibrational energy levels in Figure 2 contain the total zero-point vibrational energy of all modes rather than the vibration energy of a specific mode. The reason that the variational transition states on our potential energy surfaces are not at the saddle point is that, as  $s$  becomes negative, the increase in the zero-point energy of the C-L stretching mode is larger than the decrease in the classical potential energy and the zero-point energy of the C-L-C bending modes. The increase in the zero-point energy of the C-H stretching mode is larger than that of the C-D, and the increase in the zero-point energy of the C-T stretching mode is the smallest

of all. This produces a different variational transition state for each isotope. The quasiclassical  $k_H/k_D$  is smaller when the variational transition states are used than it would be if the saddle point were used for all three transition states. The same is true for the quasiclassical  $k_H/k_T$  and  $k_D/k_T$ . This is shown in Table I. The variational transition state values for the quasiclassical  $k_H/k_D$  and  $k_H/k_T$  for surfaces I–III and VI are smaller than the conventional transition state values. Surfaces IV and V are so steep near the saddle point that the variational transition states coincide with the conventional transition states. On these surfaces the increase in zero-point energy is smaller than the decrease in potential energy as  $s$  goes from zero to small negative values. Therefore, the two types of transition state are the same and the two theories produce the same isotope effects.

For surfaces I–VI, the values of the exponent of the Swain–Schaad relation are listed in Tables I and II for several types of calculation. The values of  $r_{qc}^*$  are all 1.47. Using a highly simplified model, without tunneling, Schaad originally obtained a value of 1.44 for  $r_{qc}^*$ .<sup>11</sup> Using a more complete quasiclassical, conventional transition state treatment, Bigeleisen suggested  $1.33 < r_{qc}^* < 1.55$ .<sup>23</sup> If quasiclassical variational transition state theory is used (no tunneling), several values well above the Bigeleisen limits are found (Table I). However, the introduction of large curvature tunneling systematically draws  $r$  back toward the original prediction (1.44)<sup>11</sup> and, with one minor exception, the  $r^{CVT}$  values again fall within the Bigeleisen limits<sup>23</sup> (Table II). However, the combination of conventional transition state theory with large curvature tunneling gives several values of  $r^*$  well below the Bigeleisen limits<sup>23</sup> (Table II). For the hydride transfer system, where the difference between the conventional transition state and the variational transition state is mainly due to zero-point energies, it is likely that the variational effect will generally raise  $r$ , because zero-point energy is largest for H (Figure 2). It has been expected that tunneling would reduce  $r$ , as it does. It is not clear to us why the same surfaces which generate large variational effects on  $r$  also generate compensating large curvature tunneling effects, nor is it certain that this will be general.

It is also sometimes of interest to relate  $k_H/k_T$  to  $k_D/k_T$  rather than to  $k_H/k_D$ . This is done in eq 1b, which is algebraically derived from eq 1a. If  $r$  is 1.44,  $r/(r-1)$  is 3.26. Values of  $r/(r-1)$  are readily obtained from all the values of  $r$  reported in this paper. It has been contended that comparison of  $k_D/k_T$  with  $k_H/k_T$  is a more sensitive way to detect deviations from the Swain–Schaad relations than comparison of  $k_H/k_D$  with  $k_H/k_T$ .<sup>24</sup> It is certainly true that the numerical value of  $r/(r-1)$  changes faster than  $r$  in the range of interest.  $(d\{r/(r-1)\}/dr = -1/(r^2 - 2r + 1); -5.17$  when  $r = 1.44$ .) However, the numerical values of  $r$  obtained from eqs 1a and 1b are identically the same. At least part of the evidence that the comparison of  $k_D/k_T$  with  $k_H/k_T$  is particularly sensitive has come from systems with more than one isotopic substitution.<sup>24</sup> These are beyond the scope of the present discussion.<sup>25</sup>

A more useful way to look for variational and tunneling effects may be to examine Arrhenius plots. Tunneling is expected to become more and more important as the temperature is reduced and the slopes of Arrhenius plots are expected to be much reduced, perhaps approaching zero values as temperature approaches 0 K.<sup>26</sup> Isotope effects are expected to become very large.<sup>26</sup> Figure 3 shows the Arrhenius plots computed from surface II with use of variational transition state theory with large curvature tunneling (eq 3a). It also shows the results without tunneling. The expected curvature occurs with either variant of transition state theory. However, with our present potential energy surfaces, curvature

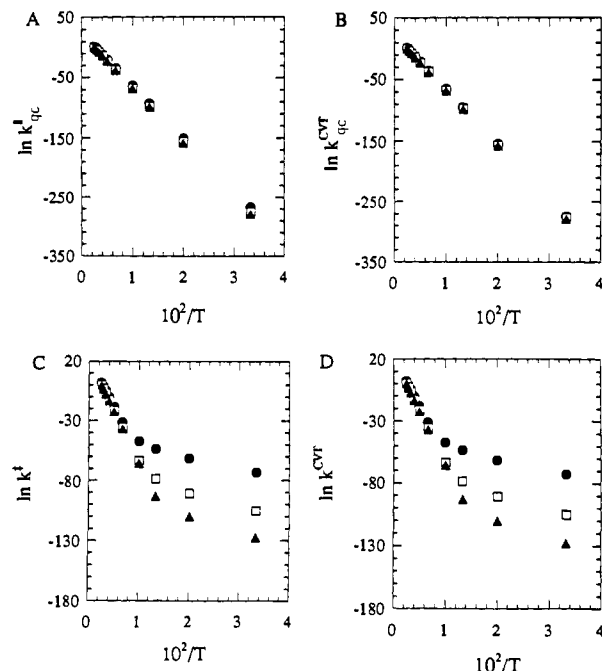


**Figure 3.** Arrhenius plots of rate constants calculated with use of surface II: (A) conventional transition state theory without tunneling; (B) variational transition state theory without tunneling; (C) conventional transition state theory with large curvature tunneling; (D) variational transition state theory with large curvature tunneling. On this scale the differences between the two types of transition state theory are barely discernable. Triangles represent T transfer, squares D transfer, and circles H transfer.

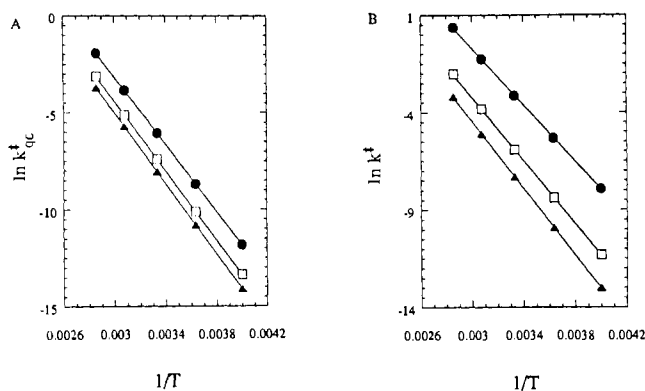


**Figure 4.** Linear least-squares fits to Arrhenius plots of rate constants calculated with use of surface V: without tunneling (A) and with tunneling (B). Because surface V has a relatively sharp maximum in its minimum energy path from reactants to products, the variational and conventional transition states are the same. Without tunneling  $E_a(D) - E_a(H) = 0.57$  kcal mol<sup>-1</sup> and  $A_H/A_D = 1.50$ . With tunneling  $E_a(D) - E_a(H) = 1.73$  kcal mol<sup>-1</sup> and  $A_H/A_D = 0.91$ . Triangles represent T transfer, squares D transfer, and circles H transfer.

only becomes readily apparent at temperatures below 100 K, which are not accessible to most experimental studies of ground-state ionic reactions in solution. However, ample experimental demonstration of this effect is available from photochemical reactions and radical reactions.<sup>26</sup> At a temperature around 300 K, with our present potential energy surfaces, curvature of the Arrhenius plots is not obvious (Figure 4). Using surface V, which maximizes the curvature, and spanning the range 250–350 K, the Arrhenius plot is not visibly curved. If  $\ln k$  is fitted to a quadratic equation in  $1/T$ , the second-order term accounts for less than 7% of its value at 300 K. It is not likely that such slight curvature can be convincingly identified with experimental rate constants, because of their scatter. Nevertheless, as has been long anticipated,<sup>2</sup> the curvature manifests itself in a significantly reduced slope and a reduced intercept if the  $\ln k$  values are fitted to a linear equation in  $1/T$ . These effects are shown in Figure 4, for surface V. The

(23) Bigeleisen, J. *Tritium in the Physical and Biological Sciences*; International Atomic Energy Agency: Vienna, 1962; p 161.

(24) Cha, Y.; Murray, C. J.; Klinman, J. P. *Science* **1989**, *243*, 1325.

(25) Huskey, W. P. *J. Phys. Org. Chem.* **1991**, *4*, 361.

(26) (a) Brunton, G.; Griller, D.; Barclay, L. R. C.; Ingold, K. U. *J. Am. Chem. Soc.* **1976**, *98*, 6803 (this paper gives many earlier references). (b) Grellmann, K. H.; Mardzinski, A.; Heinrich, A. *Chem. Phys.* **1989**, *136*, 201. (c) Al-Soufi, W.; Eychmüller, A.; Grellmann, K. H. *J. Phys. Chem.* **1991**, *95*, 2022.

**Table III.** Arrhenius Parameters ( $E_a(D) - E_a(H)$ ,  $A(H)/A(D)$ ) and  $RT$  in KIE for the Kinetic Deuterium Isotope Effect<sup>a</sup>

surface <sup>b</sup>	$E_a(D) - E_a(H)$			$A(H)/A(D)$				$RT$ ln KIE
	CVT <sup>c</sup>	CVT <sub>qc</sub> <sup>d</sup>	* <sup>e</sup>	CVT <sup>c</sup>	CVT <sub>qc</sub> <sup>d</sup>	* <sup>f</sup>	Bell <sup>g</sup>	
I	1.06	0.15	1.47	0.73	1.43	0.76	1.49	0.87
II	1.36	0.14	1.78	0.64	1.40	0.68	1.50	1.08
III	1.37	0.30	1.64	0.75	1.43	0.78	1.50	1.20
IV	1.58	0.56	1.60	0.84	1.48	0.85	1.50	1.48
V	1.73	0.57	1.73	0.91	1.50	0.91	1.51	1.67
VI	1.14	0.16	1.54	0.71	1.41	0.75	1.51	0.93

<sup>a</sup> $E_a$ 's are in kcal mol<sup>-1</sup>. The temperature range is between 250 and 350 K. <sup>b</sup>The surfaces are the same as those in Table I. <sup>c</sup>Obtained from the rate constants calculated using improved canonical variational transition state theory with large-curvature ground-state tunneling. <sup>d</sup>Same as footnote c but without tunneling. <sup>e</sup>The values without tunneling are all 0.57 for surfaces I-V and 0.56 for surface VI. <sup>f</sup>The values without tunneling are all 1.50 for surfaces I-V and 1.51 for surface VI. <sup>g</sup>Obtained using Bell's methods as described in the text (eqs 18 and 19).

distinctive consequences of tunneling appear regardless of which variant of transition state theory is used and are not obscured by variational effects.

Since tunneling is most important for H transfer it has the largest impact on the Arrhenius plot for H transfer and the least impact on the plot for T transfer. As a result  $E_a(D) - E_a(H)$  and  $E_a(T) - E_a(H)$  are raised above the values they would have had in the absence of tunneling. Since the preexponential factors,  $A$ , are determined by the intercepts of these plots,  $A_H/A_D$  and  $A_H/A_T$  are reduced below the values they would have in the absence of tunneling. These quantities are shown in Table III. Rate constants were calculated from eq 3a (variational transition state theory) with and without  $\kappa$ . The activation parameters were obtained from linear correlations of  $\ln k^{\text{CVT}}$  with  $1/T$ , over the temperature range 250–350 K. The effects are small, but large enough to be determined by careful experimental work. As the imaginary frequency and the  $\kappa$  values become larger  $E_a(D) - E_a(H)$  becomes steadily larger, and its value with and without tunneling becomes larger, mainly reflecting the increasing value of  $k_H/k_D$ . There does not appear to be any simple, general relation between  $A(H)/A(D)$  and the magnitudes of the  $k$ 's.

Unlike calculated values, experimental results are not accompanied by nontunneling reference values. To provide a reference for  $A_H/A_D$  (or  $A_H/A_T$ ) Bell<sup>2</sup> has suggested a simplified limiting model for hydrogen transfer between massive polyatomic molecules without tunneling. He used conventional transition state theory and the harmonic oscillator approximation to arrive at eqs 18 and 19,<sup>2</sup> where  $\Delta\Delta E_0$  is the double difference of zero-point energies

$$\left(\frac{k_H}{k_D}\right)_{\text{qc}}^* = \left(\frac{\mu_D^*}{\mu_H^*}\right)^{1/2} \frac{\Theta^*}{\Theta^R} \exp\left(\frac{\Delta\Delta E_0}{k_B T}\right) \quad (18)$$

$$\Theta = \prod_i \frac{u_i^H [1 - \exp(-u_i^D)]}{u_i^D [1 - \exp(-u_i^H)]} \quad (19)$$

which can be approximated by eq 15 with use of  $V_a^*$  instead of  $V_a^{\text{AG}}$ . For each vibrational frequency,  $\nu_i$ , for each species,  $u_i = h\nu_i/k_B T$ . The reduced mass in the reaction coordinate is  $\mu^*$ . If the reaction coordinate is purely hydrogenic at the transition state,  $\mu_D^*/\mu_H^*$  takes a value of 2.<sup>2</sup> (If the reaction coordinate is nonhydrogenic,  $\mu_D^*/\mu_H^*$  should be 1.0, but this limit does not interest us.) Bell assumed that there were three modes in the isotopically substituted reactant for which the vibrating mass doubled on substituting D for H, and also three such modes in the transition state. If the reaction coordinate has  $\mu_D^*/\mu_H^* = 2$ , it is one of these modes and there are only two isotopically sensitive real vibrations in the transition states.<sup>27</sup> For large molecules the translational and rotational partition functions are isotopically insensitive. If  $h\nu_i \gg k_B T$ , then  $1 - \exp(-u_i) \approx 1.0$  and each isotopically sensitive

**Table IV.** Arrhenius Parameters ( $E_a(T) - E_a(H)$ ,  $A(H)/A(T)$ ) and  $RT$  in KIE for the Kinetic Tritium Isotope Effect<sup>a</sup>

surface <sup>b</sup>	$E_a(T) - E_a(H)$			$A(H)/A(T)$				$RT$ ln KIE
	CVT <sup>c</sup>	CVT <sub>qc</sub> <sup>d</sup>	<sup>e</sup>	CVT <sup>c</sup>	CVT <sub>qc</sub> <sup>c</sup>	<sup>f</sup>	Bell <sup>g</sup>	
I	1.30	0.27	1.88	0.76	1.68	0.82	1.74	1.14
II	1.69	0.40	2.14	0.72	1.67	0.77	1.74	1.50
III	1.85	0.58	2.11	0.82	1.71	0.85	1.74	1.73
IV	2.26	0.83	2.27	0.87	1.77	0.88	1.74	2.17
V	2.66	0.84	2.66	0.77	1.79	0.77	1.74	2.50
VI	1.45	0.35	1.93	0.78	1.70	0.82	1.75	1.30

<sup>a</sup> $E_a$ 's are in kcal mol<sup>-1</sup>. The temperature range is between 250 and 350 K. <sup>b</sup>The surfaces are the same as those in Table I. <sup>c</sup>Obtained from the rate constants calculated using improved canonical variational transition state theory with large-curvature ground-state tunneling. <sup>d</sup>Same as footnote c but without tunneling. <sup>e</sup>The values without tunneling are all 0.85 for surfaces I-V and 0.83 for surface VI. <sup>f</sup>The values without tunneling are all 1.79 for surfaces I-V and 1.80 for surface VI. <sup>g</sup>Obtained using Bell's methods as described in the text (eqs 18 and 19).

vibration contributes a factor of  $2^{1/2}$  to  $\Theta$ . If  $h\nu_i \ll k_B T$ , the system behaves classically and all vibrational partition functions are equal. Taking the former approximation for the reactants Bell obtained a value of  $2^{3/2}$  for  $\Theta^R$ . By taking the latter approximation for the transition state he obtained unity for  $\Theta^*$ . Identifying the combined preexponential factors with  $A$ , a minimum value of  $1/2$  is obtained. In the high-temperature limit,  $h\nu_i \ll k_B T$ , and a maximum value of 1.4 is given for  $(k_H/k_D)_{\text{qc}}^*$  by  $(\mu_D^*/\mu_H^*)^{1/2}$ .<sup>2</sup> Within the context of conventional transition state theory, a good case can be made that these limits are conservatively broad, because it is unlikely that  $h\nu_i \gg k_B T$  for the reactant and  $h\nu_i \ll k_B T$  for the transition state, so the quasiclassical  $A$  values should be close to unity.<sup>28,29</sup> To test the usefulness of these limiting reference values, suitably adapted versions of eqs 18 and 19 have been applied to the present case.

For the reactants in the triatomic case there is only one isotopically sensitive vibration, so  $\Theta^R = 2^{1/2}$ . Following Bell's prescription for the transition state,  $\Theta^* = 1.0$ . Since  $\mu_D^*/\mu_H^*$  is 2, the lower limiting value of  $A_H/A_D$  is 1.0. The upper (high temperature) limit is just  $(\mu_D^*/\mu_H^*)^{1/2} = 2^{1/2}$ . As shown in Table III, in the absence of tunneling the values of  $A_H/A_D$  obtained from the Arrhenius plots made with either the  $k^*$  or the  $k^{\text{CVT}}$  values are close to or above the upper limit, and the (almost invariant) conventional transition state value, 1.5, is similar to the values given by variational transition state theory. The saddle point bending frequencies are 837, 603, and 500 cm<sup>-1</sup> respectively for H, D, and T. The values at the variational transition state are somewhat smaller. In the temperature range of interest, these  $h\nu_i$  are neither much greater nor much smaller than  $k_B T$ , but the former is much more nearly true than the latter. If  $h\nu_i \gg k_B T$  and  $1 - \exp(-u_i) \approx 1.0$  are assumed for the transition state as well as the reactant,  $\Theta^* \approx 2.0$  and  $A_H/A_D \approx 2.0$ . The values of  $A_H/A_D$  obtained without tunneling are all below this estimate. The introduction of tunneling further reduces the  $A_H/A_D$  values by a factor of about 2, but they are only marginally below the lower limit of quasiclassical effects obtained from the Bell model. The tritium isotope effects, analyzed in Table IV, yield similar conclusions. We conclude that the Bell model and the limits on  $A_H/A_D$  obtained from it are not realistic enough to be useful. Most cases of shallow tunneling will go undetected. However, we believe that the foregoing analysis suggests an attractive alternative. The triatomic system is atypical in that it has no isotopically sensitive bending frequencies in the reactants. This exaggerates the effect of the bending frequencies in the transition state, because they are uncompensated. For the general case, therefore, a reasonable approximation would seem to be that all  $h\nu_i \gg k_B T$  so that all  $1 - \exp(-u_i) \approx 1.0$ . The approximation  $h\nu_i \gg k_B T$  will be inexact to about the same degree in reactants and the transition state so

(28) Melander, L.; Saunders, W. H., Jr. *Reaction Rates of Isotopic Molecules*; John Wiley and Sons: New York, 1980; pp 144–147.

(29) (a) Schneider, M. E.; Stern, M. J. *J. Am. Chem. Soc.* 1972, 94, 1517. (b) Stern, M. J.; Weston, R. E. *J. Chem. Phys.* 1974, 60, 2808.

it should lead to approximately correct values of  $A_H/A_D$ . In this way  $A_H/A_D \approx 1.0$  is obtained for the general case of massive, polyatomic molecules in the absence of tunneling. This value also has considerable support in the detailed calculations of Schneider and Stern<sup>29a</sup> and Stern and Weston.<sup>29b</sup> It should be valid in the absence of low-frequency, uncompensated, isotopically-sensitive vibrations in the reactants or transition state. The only large class of such vibrations that comes to mind is restricted rotations. For hydrogen transfer reactions of massive, polyatomic molecules we believe that  $A_H/A_D$  values (or  $A_H/A_T$  values) substantially less than 1.0, reliably obtained from rate constants between 250 and 350 K, can be taken as suggestive of tunneling. We do not propose these values as a lower limit of quasiclassical  $A_H/A_D$  values, below which tunneling is proved. Because of the approximations built into transition state theory and because it is impossible to generalize reliably about hyperdimensional potential surfaces, and, therefore, impossible to generalize reliably about the vibrational partition functions, we do not believe that any reliable and useful limit can be obtained. Any limit low enough to be reliable would fail to identify most examples of shallow tunneling. We believe that our suggested criterion for tunneling,  $A_H/A_D < 1.0$  by an amount safely outside of experimental uncertainty, will correctly distinguish tunneling from nontunneling processes in most cases. When this estimate is adapted to the triatomic cases it gives  $A_H/A_D \approx 2.0$ , and this would misidentify the quasiclassical rate constants with shallow tunneling processes. However, as pointed out above, the triatomic system is atypical because of the uncompensated bending frequencies in the transition states. Values of  $E_a(D) - E_a(H)$  larger than 1.35<sup>2</sup> or larger than 1.20<sup>28</sup> kcal mol<sup>-1</sup> have been suggested as criteria of tunneling, because these values would result from the loss of zero-point energy in one hydrogenic stretching mode. The corresponding values for  $E_a(T) - E_a(H)$  are 2.0 and 1.8 kcal mol<sup>-1</sup>. Tables III and IV show that the  $E_a(D) - E_a(H)$  values and the  $E_a(T) - E_a(H)$  values obtained from the triatomic system, with tunneling, for most of our systems fail to meet or just barely meet this criterion. However, the uncompensated bending modes lower the  $E_a(D) - E_a(H)$  values by  $\sim 0.5$  kcal mol<sup>-1</sup>. If 0.5 kcal mol<sup>-1</sup> is added to the tabulated  $E_a(D) - E_a(H)$  values, all but that from the first surface meet the criterion and all the  $E_a(D) - E_a(H)$  values obtained from quasiclassical rate constants fall short. The values of  $E_a(D) - E_a(H)$  increase as tunneling becomes more important. The KIE also increases as tunneling becomes more important, and the increase in  $RT \ln(k_H/k_D)$  just about equals the increase in  $E_a(D) - E_a(H)$ . We, therefore, believe that  $E_a(D) - E_a(H) > 1.20$  kcal mol<sup>-1</sup> (or  $E_a(T) - E_a(H) > 1.8$  kcal mol<sup>-1</sup>) for hydrogen transfer between massive polyatomic molecules should be regarded as suggestive of tunneling. If both criteria are met,  $E_a(D) - E_a(H) > 1.20$  kcal mol<sup>-1</sup> and  $A_H/A_D < 1.0$ , we believe the case for tunneling is quite strong. These conclusions are essentially the same as those reached previously by Melander and Saunders,<sup>28</sup> from a rather different model. As an example, these criteria can be applied to a recent collection of results on hydrogen atom transfer from toluene to diarylcarbenes at temperatures centering a little above 300 K.<sup>30</sup> Eight substances were studied. For five of them, with  $k_H/k_D$  between 8.4 and 5.3,  $E_a(D) - E_a(H)$  was significantly above 1.2. These same five reactions gave  $A_H/A_D$  values between 0.3 and 0.6. We would classify all five as cases of shallow, corner-cutting tunneling. The original authors classified three of these in the same way, but were doubtful about two.<sup>30</sup> One value of  $E_a(D) - E_a(H)$  was 1.2 with an  $A_H/A_D$  of 0.75. We would regard this as a borderline case, as did the original authors,<sup>30</sup> even though  $k_H/k_D = 5.6$ . Two cases, with  $k_H/k_D$  values of 4.1 and 6.1, give  $E_a(D) - E_a(H)$  values below 1.0.<sup>30</sup> These also gave  $A_H/A_D$  values above 1.0.<sup>30</sup> The original authors saw no evidence of tunneling,<sup>30</sup> and we agree. A very clear case of tunneling is presented by the enzymatic oxidation of benzylamine.<sup>31</sup> The  $k_H/k_T$  is 35.2 at 25 °C (equivalent to  $k_H/k_D = 11.9$  if eq 1a is applied with  $r = 1.44$ ),

Table V. Experimental  $E_a(D) - E_a(H)$  and  $A_H/A_D$  Values

reaction	solvent	KIE <sup>a</sup>	$A(H)/A(D)$	$E_a(D) - E_a(H)$	ref
4-NPNM <sup>b</sup> + Et <sub>3</sub> N	CH <sub>3</sub> CN	3.12	0.55	1.02	32
4-NPNM + <i>n</i> -Bu <sub>3</sub> N	CH <sub>3</sub> CN	2.17	0.60	0.74	32
2-CECP <sup>c</sup> + D <sub>2</sub> O	D <sub>2</sub> O	3.42	0.44	1.21	33
2-CECP + CH <sub>2</sub> ClCO <sub>2</sub> <sup>-</sup>	D <sub>2</sub> O	3.70	0.35	1.45	33
2-CECP + F <sup>-</sup>	D <sub>2</sub> O	2.66	0.04	2.44	33

<sup>a</sup> At 298 K. <sup>b</sup> (4-Nitrophenyl)nitromethane. <sup>c</sup> 2-Carboethoxycyclopentanone.

$E_a(T) - E_a(H)$  is 3.4 kcal mol<sup>-1</sup>, and  $A_H/A_D = 0.12$ .<sup>31</sup> It is noteworthy that a value of 1.46 is nevertheless obtainable for the Swain-Schaad  $r$ .<sup>31</sup>

Since the  $E_a$  values and the  $A$  values will presumably come from the same Arrhenius plots, the criterion based on an  $E_a$  value should generally be correlated with that based on  $A$  values. Both may occasionally identify tunneling in questionable cases. There exist a number of reactions for which  $A_H/A_D$  suggests tunneling,  $E_a(D) - E_a(H)$  is around 1.2 kcal mol<sup>-1</sup>, but  $k_H/k_D$  is quite modest. A selection of these is shown in Table V. Tables III and IV show that  $E_a(D) - E_a(H)$  and  $E_a(T) - E_a(H)$  are often systematically reduced by variational effects. The origin of this effect has been discussed above. This may sometimes account for such observations. The reactions of 2-carboethoxycyclopentanone with D<sub>2</sub>O and chloroacetate may well be such cases.

Unsuspected mechanistic complexity may be involved in other cases of disagreement between the  $A_H/A_D$  criterion and the  $E_a(D) - E_a(H)$  criterion. For example, the reactions of (4-nitrophenyl)nitromethane with tertiary amines in acetonitrile produces, in its first stage, an ion pair hydrogen bonded at the anionic carbon. The final product ion pair is probably hydrogen bonded at one of the nitronate oxygens. The original authors believed that the product ion pair was undissociated, but the experiments which lead to this conclusion were performed on more concentrated solutions than those in which kinetic measurements were made.<sup>32</sup> It seems quite possible that a significant fraction of free ions was formed in the kinetic experiments. It, therefore, seems quite possible that the rearrangement and/or separation of the initially formed product may be partially rate limiting. This would certainly reduce the isotope effect and  $E_a(D) - E_a(H)$ . Its effect on  $A_H/A_D$  is not easy to foresee.

We see no explanation for the value of  $A_H/A_D$  obtained from the reaction of 2-carboethoxycyclopentanone with fluoride.<sup>33</sup> The reaction appears to merit further examination.

Next we examine the effect of varying the equilibrium donor-acceptor separation while holding all other potential parameters constant. Lewis showed<sup>34</sup> and others have confirmed<sup>35</sup> that the introduction of bulky substituents close to the site of a proton transfer leads to an increase in the KIE, which can be substantial.<sup>34,35</sup> It has been thought that this increase is due to tunneling, brought about because steric repulsion leads to a "narrow" barrier.<sup>34,35</sup> In our earlier papers,<sup>3,14</sup> we have pointed out that corner-cutting, shallow tunneling could account for the observed effects without imposing any special constraints on the shape of the barrier. The introduction of bulky substituents would have the effect of changing the equilibrium donor-acceptor distance, so that by examining the result of such changes in our model we hope to elucidate the origin of steric increases in the KIE. Tables VI-IX show the effect of changes in the equilibrium donor-acceptor distance on the characteristics of the transition states and the kinetic parameters at or near 300 K. In all cases a high proportion of the hydrogen transfer events occur by tunneling. As before, however, this is shallow corner-cutting, allowing the

(32) Caldin, E. F.; Jarczewski, A.; Lefk, K. T. *Trans. Faraday Soc.* **1971**, *67*, 110.

(33) Bell, R. P.; Fendley, J. A.; Hulett, J. R. *Proc. R. Soc. London, A* **1956**, *235*, 453.

(34) Lewis, E. S.; Funderburk, L. H. *J. Am. Chem. Soc.* **1967**, *89*, 2322.

(35) Melander, L.; Saunders, W. H., Jr. *Reaction Rates of Isotopic Molecules*; John Wiley and Sons: New York, 1980; p 152.

(30) Shaffer, M. W.; Leyva, E.; Soundararajan, N.; Chang, E.; Chang, D. H. S.; Capuano, V.; Platz, M. S. *J. Phys. Chem.* **1991**, *95*, 7273.

(31) Grant, K. L.; Klinman, J. P. *Biochemistry* **1989**, *28*, 6597.

**Table VI.** Conventional and Variational Transition State Theory Potential Energy Surface Properties and Quasiclassical Rate Constants for Potential Energy Surface II with Different Donor–Acceptor Equilibrium Distances at 300 K

$R_e(\text{C}-\text{C}), \text{\AA}$	$V_i(\text{H}),^a \text{cm}^{-1}$	$V_b^*(\text{H}),^b \text{cm}^{-1}$	$10^5 k_{\text{H}}^c, \text{M}^{-1} \text{s}^{-1}$	$10^5 k_{\text{H}}^{\text{CVT},d} \text{M}^{-1} \text{s}^{-1}$	$10^5 k_{\text{D}}^c, \text{M}^{-1} \text{s}^{-1}$	$10^5 k_{\text{D}}^{\text{CVT},d} \text{M}^{-1} \text{s}^{-1}$	KIE <sub>qc</sub>	KIE <sub>qc</sub> <sup>CVT</sup>
3.228	989	837	239.0	106.6	61.17	59.87	3.91	1.78
3.254	1118	836	23.89	14.11	61.11	6.111	3.91	2.31
3.281	1234	835	2.255	1.997	0.576	0.576	3.91	3.41
3.307	1342	833	0.202	0.202	0.052	0.052	3.91	3.91

<sup>a</sup>The imaginary frequency at the saddle point, with H as the transferred atom. Within a few percent,  $V_i(\text{D})$  and  $V_i(\text{T})$  are given by  $(\mu_{\text{H}}/\mu_{\text{L}})^{1/2} V_i(\text{H})$ , where  $\mu_{\text{L}}$  is the reduced mass of A–L, with an atomic weight of 15 daltons for A and a mass of 1, 2, or 3 daltons for L. <sup>b</sup>The bending frequency at the saddle point. <sup>c</sup>Calculated from eq 3b, omitting  $\kappa$ . <sup>d</sup>Calculated from eq 3q, omitting  $\kappa$ .

**Table VII.** Transmission Coefficients, Percentages of Tunneling, and KIE Values for Potential Energy Surface II with Different Donor–Acceptor Equilibrium Distances at 300 K<sup>a</sup>

$R_e(\text{C}-\text{C})$	$R_{\text{H}}^{\text{CC}}(\text{CC})^b$	$R_{\text{D}}^{\text{CC}}(\text{CC})^c$	$\kappa_{\text{H}}$	$P_{\text{T}}^{\text{H}}$	$\kappa_{\text{D}}$	$P_{\text{T}}^{\text{D}}$	KIE	KIE <sup>CVT</sup>
3.228	3.050	3.004	5.32	91	1.54	56	13.5	6.15
3.254	3.053	3.014	9.07	95	2.27	71	15.6	9.23
3.281	3.062	3.016	21.2	96	3.26	80	25.4	22.6
3.307	3.070	3.042	26.0	98	3.86	82	26.3	26.3

<sup>a</sup>All distances are in  $\text{\AA}$ . The surfaces are the same as those generating Table VI. <sup>b</sup>The C–C distance at the critical configuration for hydride transfer. <sup>c</sup>The C–C distance at the critical configuration for deuteride transfer.

**Table VIII.** Arrhenius Parameters ( $E_a(\text{D}) - E_a(\text{H})$ ,  $A(\text{H})/A(\text{D})$ ) and  $RT \ln$  KIE for Surface II with Different Equilibrium Donor–Acceptor Distances<sup>a</sup>

$R_e(\text{C}-\text{C}), \text{\AA}$	$E_a(\text{D}) - E_a(\text{H})$				$A(\text{H})/A(\text{D})$				$RT \ln$ KIE
	CVT <sup>b</sup>	CVT <sub>qc</sub> <sup>c</sup>	* <sup>d</sup>	* <sup>e</sup>	CVT <sup>b</sup>	CVT <sup>c</sup>	* <sup>e</sup>	Bell <sup>f</sup>	
3.338	1.36	0.14	1.78	0.64	1.40	0.68	1.50	1.08	
3.254	1.61	0.29	1.89	0.62	1.42	0.65	1.49	1.32	
3.281	1.81	0.51	1.86	0.63	1.45	0.65	1.50	1.53	
3.307	2.25	0.57	2.25	0.61	1.50	0.61	1.49	1.95	

<sup>a</sup> $E_a$ 's are in kcal mol<sup>-1</sup>. The temperature range is between 250 and 350 K. <sup>b</sup>Obtained from the rate constants calculated using improved canonical variational transition state theory with large-curvature ground-state tunneling. <sup>c</sup>Same as footnote b but without tunneling. <sup>d</sup>The values without tunneling are all 0.57. <sup>e</sup>The values without tunneling are all 1.50. <sup>f</sup>Obtained using Bell's methods as described in the text (eqs 18 and 19). <sup>g</sup>The surfaces are the same as those used in Table VI.

**Table IX.** The Exponents in the Swain–Schaad Relationship for Surface II with Different Donor–Acceptor Equilibrium Distances at 300 K<sup>a</sup>

$R_e(\text{C}-\text{C})$	$r_{\text{qc}}^*$	$r_{\text{qc}}^{\text{CVT}}$	$r^*$	$r^*$	$r^{\text{CVT}}$
3.228	1.47	2.08	1.06	1.27	1.38
3.254	1.47	1.77	1.18	1.32	1.40
3.281	1.47	1.52	1.42	1.45	1.47
3.307	1.48	1.48	1.36	1.41	1.41

<sup>a</sup>The  $r$  values were obtained in the same way as described in Tables I and II. The surfaces are the same as those used in Table VI. All distances are in  $\text{\AA}$ .

reactions to evade only a small fraction of the activation barrier. At 300 K hydrogen transfer rate constants are increased by factors between 5 and 26. Even for deuterium transfer tunneling is significant in all cases at 300 K. Again, however, clear evidence for the role of tunneling would be hard to extract from experimental results. The results with tritium, not tabulated, follow the same pattern.

As anticipated,<sup>34,35</sup>  $k_{\text{H}}/k_{\text{D}}$  increases considerably as the donor–acceptor distance increases. However, variational transition state theory shows that the increase is not entirely due to tunneling. The quasiclassical contribution to  $k_{\text{H}}/k_{\text{D}}$  also increases with increasing donor–acceptor distance. The transition state for hydrogen transfer and those for deuterium and tritium transfer become increasingly similar as the donor–acceptor distance is increased, and the imaginary frequency at the saddle point increases. This increases both the tunneling and the quasiclassical KIE values. Thus, an increase in  $k_{\text{H}}/k_{\text{D}}$  with increasing steric hindrance to reaction is consistent with tunneling in both hindered and unhindered cases and does not require the attribution of any

special shape to the barrier. However, an increase in  $k_{\text{H}}/k_{\text{D}}$  with increasing steric hindrance does not uniquely identify tunneling, and other indications of tunneling are needed.

The Swain–Schaad ratios (Table IX) behave as they do when the widening function is varied. The variational, quasiclassical ratios vary considerably, but when tunneling is taken into account, the final predicted values all lie within the 1.33–1.50 range. In fact, it is the variational, quasiclassical ratios *without* tunneling which give anomalous Swain–Schaad ratios (too large). If only one isotopic substitution is made the Swain–Schaad relation is probably quite reliable for calculating one hydrogen isotope effect from another, but apparently it will not help to identify tunneling. This is the same conclusion reached by Stern and Weston,<sup>36</sup> who considered tunneling through a one-dimensional Eckart barrier, and Melander and Saunders,<sup>28</sup> who used a one-dimensional parabolic barrier. It is not an artifact of a particular barrier shape. Tunneling may lead to  $r$  values outside of the expected limits in systems with more than one isotopically sensitive hydrogen,<sup>24</sup> but such an outcome apparently requires other conditions to be met as well,<sup>25,31</sup> and such systems are beyond the scope of the present paper.

If, as suggested above, 0.5 kcal mol<sup>-1</sup> is added to each of the  $E_a(\text{D}) - E_a(\text{H})$  values in Table VIII, all the values from calculations with tunneling are well above 1.20 kcal mol<sup>-1</sup>, correctly signaling tunneling. Helpfully, the  $E_a(\text{D}) - E_a(\text{H})$  values increase as tunneling becomes more important, as they also do when the widening function is varied. This increase parallels the increase in  $RT \ln (k_{\text{H}}/k_{\text{D}})$ . All the values from calculations without tunneling are below 1.20 kcal mol<sup>-1</sup>, but at the larger donor–acceptor separations they are close enough after addition of 0.5 kcal mol<sup>-1</sup> that experimental error might confuse the result if we were dealing with real experimental data. Once again, the values of  $A(\text{H})/A(\text{D})$  do not appear to change with the magnitudes of the  $k$ 's, although all are low enough to meet our criterion for the probable occurrence of tunneling.

Finally, we recall that, in earlier work,<sup>3,13,14</sup> we have suggested that the variation of  $k_{\text{H}}/k_{\text{D}}$  with the variation of the reaction equilibrium constant,  $K_{\text{eq}}$ , could be used to identify shallow, corner-cutting tunneling if  $K_{\text{eq}}$  is not far from unity. With  $K_{\text{eq}} > 1$ , if the structural changes which increase  $K_{\text{eq}}$  are in the hydrogen acceptor,  $k_{\text{H}}/k_{\text{D}}$  should decrease as  $K_{\text{eq}}$  increases; but  $k_{\text{H}}/k_{\text{D}}$  should increase as  $K_{\text{eq}}$  increases if the structural changes are in the hydrogen donor.<sup>3,14</sup> The anticipated changes are modest, but measurable, with care, in favorable systems.<sup>13,14</sup> This prediction is based on the expectation that the donor–acceptor distance in the critical configuration for hydrogen tunneling will be greater than that for deuterium tunneling. Tables VI and VII show that

the donor-acceptor distances behave as expected.

#### 4. Conclusions

Shallow, corner-cutting tunneling is very wide spread in hydrogen transfer reactions. It is intrinsic to quantum mechanisms, just as zero-point energy is.<sup>37</sup> In the present and previous<sup>3,14</sup> calculations its effect on hydrogen transfer rate constants for temperatures around 300 K have usually been only a factor of about 10 and never as high as 10<sup>2</sup>. If these calculations approximate reality, as we believe they do,<sup>14</sup> tunneling only changes the Gibbs free energy of activation by 5-10%. Nevertheless, it usually accounts for around half of the primary hydrogen isotope effect.

The exponent of the Swain-Schaad relation cannot give information about the importance of tunneling in systems with only one isotopically sensitive hydrogen. The exponent is usually within the 1.33-1.55 range even though the tunneling correction is significant. In addition to this, the variational effect can lead to a larger value of the exponent than 1.55 without tunneling. In fact, the tunneling effect has a tendency to bring the exponent of the Swain-Schaad relation back within the expected range when the variational effect makes it large. The Swain-Schaad relation

(37) Bell, R. P. *The Tunnel Effect in Chemistry*; Chapman and Hall: New York, 1980; pp 1-11.

seems to be a reliable way to approximate a tritium isotope effect from the corresponding deuterium isotope effect, and vice versa.

On the basis of rate constants measured around 300 K, values of  $E_a(D) - E_a(H)$  greater than 1.20 kcal mol<sup>-1</sup> will usually signal tunneling as will values of  $A_H/A_D < 1.0$  for hydrogen transfer between massive, polyatomic donors and acceptors. When both characteristics are present they are strong evidence of tunneling, but they cannot be described as completely definitive.

A particular pattern of the variation of  $k_H/k_D$  with changes in donor and acceptor structures and  $K_{eq}$ , described previously and above, can sometimes provide very strong evidence of shallow, corner-cutting tunneling.

There probably is no completely unambiguous way to demonstrate shallow, corner-cutting tunneling for reactions carried out around 300 K. Such evidence is only available at much lower temperatures, where deep tunneling becomes prevalent and rate constants for hydrogen transfer reactions approach temperature independence. However, models incorporating tunneling will generally provide a more accurate understanding of experimental observations than those which do not.

**Acknowledgment.** We thank Prof. D. G. Truhlar, Dr. T. N. Truong, Dr. Da-Hong Lu, Dr. B. C. Garrett, and Dr. T. Joseph for the use of the POLYRATE program and for their generous help and encouragement.

## Covalent Bond Lengthening in Hydroxyl Groups Involved in Three-Center and in Cooperative Hydrogen Bonds. Analysis of Low-Temperature Neutron Diffraction Data

Thomas Steiner and Wolfram Saenger\*

Contribution from the Institut für Kristallographie, Freie Universität Berlin, Takustrasse 6, W-1000 Berlin 33, Germany. Received December 6, 1991

**Abstract:** The lengthening of the covalent O-D bond  $d_{O-D}$  in O-D...O hydrogen-bonding hydroxyl groups is studied from low-temperature, high-resolution neutron diffraction data of two  $\beta$ -cyclodextrin complexes (all O-D groups deuterated). The focus is primarily on the long-distance region of the hydrogen bond length D...O ( $d_{D...O}$ ). The slope of the regression line  $d_{O-D}$  versus  $d_{D...O}$  does not become 0, and an asymptotic value of  $d_{O-D}$  for an unperturbed hydroxyl group is not reached even for long distances of  $d_{D...O} \sim 2.1$  Å. This may be taken as an experimental indication for the long-range interaction of the hydrogen bond, which decreases very smoothly. An influence of three-center hydrogen bonding and of cooperativity on the O-D bond length is clearly observed. In three-center bonds, the formation of a minor hydrogen bond component  $< 2.4$  Å lengthens the O-D bond by  $\sim 0.01$  Å in addition to the lengthening by the major component. In chains of hydrogen-bonded O-D groups, the cooperative effect lengthens the O-D bond also by  $\sim 0.01$  Å if the D...O distance is  $< 1.8$  Å.

#### Introduction

It was recognized early from neutron diffraction experiments that in O-H...O hydrogen bonds (H-bonds), the covalent O-H bond ( $d_{OH}$ ) is lengthened with shortening H-bond distance  $d_{H...O}$  (or  $d_{O...O}$ ),<sup>1</sup> correlation plots of  $d_{OH}$  versus  $d_{O...O}$  and  $d_{H...O}$  derived from neutron diffraction data have repeatedly been shown.<sup>2-6</sup>

General interest has focused primarily on short hydrogen bonds with  $d_{H...O} < 1.7$  Å, for which the lengthening of  $d_{OH}$  is considerable; in the extreme case, the H atom may be placed exactly between two O atoms ("symmetric" hydrogen bonds with  $d_{O...O} \sim 2.4$  Å and  $d_{OH} \sim 1.2$  Å). Short distances  $d_{H...O} < 1.7$  Å are, however, only observed if the donor or the acceptor group is an ion, and in intramolecular H-bonds with sterically constrained, short O...O separations.<sup>6</sup> For longer H-bonds with  $d_{H...O} > 1.7$  Å, the lengthening of  $d_{OH}$  has not been explored as extensively. For the special case of water donors, a correlation plot between  $d_{OH}$  and  $d_{H...O}$  for the region  $1.6$  Å  $< d_{H...O} < 2.2$  Å shows that  $d_{OH}$  decreases with increasing  $d_{H...O}$  even for the longest H...O separations considered.<sup>5</sup> This suggests that  $d_{OH}$  should be slightly

(1) Peterson, S. W.; Levy, H. A.; Simonsen, S. H. *J. Chem. Phys.* **1953**, *21*, 2084-2085.

(2) Nakamoto, K.; Margoshes, M.; Rundle, R. E. *J. Am. Chem. Soc.* **1955**, *77*, 6480-6486.

(3) Pimentel, G. C.; McClellan, A. L. *Annu. Rev. Phys. Chem.* **1971**, *22*, 347-385.

(4) Olovsson, I.; Jönsson, P.-G. In *The Hydrogen Bond, Recent Developments in Theory and Experiments*; Schuster, P., Zundel, G., Sandorfy, C., Eds.; North-Holland: Amsterdam, 1976; pp 394-455.

(5) Chiari, G.; Ferraris, G. *Acta Crystallogr., Sect. B* **1982**, *B38*, 2331-2341.

(6) Jeffrey, G. A.; Saenger, W. *Hydrogen Bonding in Biological Structures*; Springer: Berlin, 1991.